NASA-CR-167494

ARL-TR-81-51

Copy No. 2

DIGITAL CORRELATION OF DDRS DATA

Final Technical Report under Contract NAS9-16208

Carroll R. Griffin
James M. Estes

APPLIED RESEARCH LABORATORIES
THE UNIVERSITY OF TEXAS AT AUSTIN
POST OFFICE BOX 8029, AUSTIN, TEXAS 78712

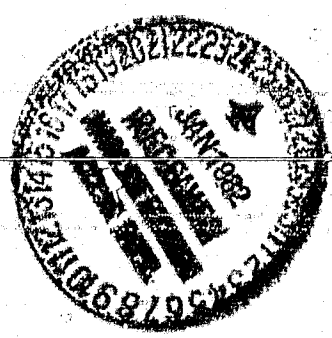

24 November 1981

Final Report

1 October 1980 - 30 September 1981

Prepared for:

NATIONAL AERONAUTICS AND SPACE ADMINISTRATION
LYNDON B. JOHNSON SPACE CENTER
HOUSTON, TX 77058

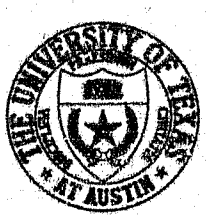

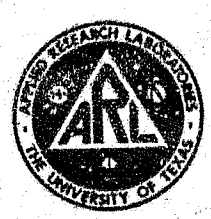

UNCLASSIFIED

SECURITY CLASSIFICATION OF THIS PAGE (When Data Entered)

REPORT DOCUMENTATION PAGE		READ INSTRUCTIONS BEFORE COMPLETING FORM
1. REPORT NUMBER	2. GOVT ACCESSION NO.	3. RECIPIENT'S CATALOG NUMBER
4. TITLE (and Subtitle) DIGITAL CORRELATION OF DDRS DATA		5. TYPE OF REPORT & PERIOD COVERED Final Report 1 Oct 80 - 30 Sep 81
		6. PERFORMING ORG. REPORT NUMBER ARL-TR-81-51
7. AUTHOR(s) Carroll R. Griffin James M. Estes		8. CONTRACT OR GRANT NUMBER(s) NAS9-16208
9. PERFORMING ORGANIZATION NAME AND ADDRESS Applied Research Laboratories The University of Texas at Austin Austin, Texas 78712		10. PROGRAM ELEMENT, PROJECT, TASK AREA & WORK UNIT NUMBERS
11. CONTROLLING OFFICE NAME AND ADDRESS National Aeronautics and Space Administration Lyndon B. Johnson Space Center Houston, Texas 77058		12. REPORT DATE 24 November 1981 13. NUMBER OF PAGES 43
14. MONITORING AGENCY NAME & ADDRESS(if different from Controlling Office)		15. SECURITY CLASS. (of this report) UNCLASSIFIED 15a. DECLASSIFICATION/DOWNGRADING SCHEDULE N/A

16. DISTRIBUTION STATEMENT (of this Report)

17. DISTRIBUTION STATEMENT (of the abstract entered in Block 20, if different from Report)

18. SUPPLEMENTARY NOTES

19. KEY WORDS (Continue on reverse side if necessary and identify by block number)

Synthetic aperture radar
SAR processing
Digital radar signal processing

20. ABSTRACT (Continue on reverse side if necessary and identify by block number)

This report details efforts under two phases of an effort to assist NASA/JSC in the reduction of digital SAR (synthetic aperture radar) data to radar images for use in remote sensing applications. The actual reduction of data was deleted and the responsibility assigned to the operating contractor. The second phase, to assist the operating contractor to achieve the data reduction capability, is the subject of the report. The critical software operations are discussed in detail, and suggestions and recommendations are made for use by NASA and the operating contractor in improving the algorithms currently being used.

DD FORM 1 JAN 73 1473 EDITION OF 1 NOV 65 IS OBSOLETE

UNCLASSIFIED

SECURITY CLASSIFICATION OF THIS PAGE (When Data Entered)

TABLE OF CONTENTS

LIST OF FIGURES

I. BACKGROUND AND OBJECTIVES

A. Background

Under Contract NAS9-16104, Applied Research Laboratories, The University of Texas at Austin (ARL:UT), was tasked to develop the software required to correlate object scene radar video data from the APQ-102 radar system. The compressed pulse video data are sampled, digitized, and recorded on a wideband tape recorder in the aircraft testbed.

Since the recording format was designed to be compatible with reformatting equipment available at ARL:UT (the digital recording interface equipment, or DRIE), it was planned to ship all the recorded data to ARL:UT so that the image formation algorithms could be developed and the data processed into high resolution radar images.

A longer term objective of NASA/JSC was to establish the capability for reformatting and processing the raw data tapes in their own facility but, in the interim, to obtain support from ARL:UT for processing user requested radar data. The contractual effort under Contract NAS9-16208 was, therefore, to perform two principal tasks.

1. Reformat and correlate selected radar scene data obtained with the APQ-102 radar and digital data recording system (DDRS), up to a maximum of five images.
2. Transfer the requisite information for performing the above tasks to NASA's operating contractor, thus establishing the capability to complete all data gathering and image generation and display tasks within the JSC organization.

At the time the contract was initiated, some delay had been experienced in developing the software for use on the DDRS data due, principally, to lack of DDRS data with which to test the algorithms and verify the software. Eventually, NASA's contractor was able to check out and render operational the DDRS, but the first of the wideband tapes was not provided until the end of October, one month after the contract start date. Eventually, the software was developed, but the second objective, educating and assisting NASA in the development of an internal capability, was carried on simultaneously.

As a result, when data tapes were finally being generated for program investigators, an initial capability had been achieved at NASA to generate the images. A decision was made not to supply those tapes to ARL:UT for correlation, but instead to have ARL:UT concentrate on refining the software algorithms and assisting JSC in achieving a full in-house data processing capability.

B. Objectives

Aside from the canceled objective of actually reducing data for five images and supplying the results to NASA, efforts were made to achieve a final transfer of the software algorithms to NASA/JSC for implementation on the VAX computer system obtained for the purpose. Combined with an array processor, the computer gives NASA's contractor a powerful tool for the reformatting and processing operations.

The theory and procedures for image formation were to be conveyed to both NASA and Lockheed personnel in tutorial sessions. It was intended that the specific algorithms developed by ARL:UT be employed by Lockheed; however, once the theory was grasped, several nontrivial efforts were mounted independently at NASA to process the data from APQ-102 data gathering flights using software developed from algorithms based on the theory of synthetic aperture radar.

Unfortunately, the program and subroutines that evolved produced images of relatively low quality, i.e., they were poorly registered or were blurred. ARL:UT's efforts to analyze the problems were unsuccessful due to inadequate liaison with both NASA and Lockheed personnel, toward the end of the contract. In summary, additional work is needed to investigate the problems with the processing software developed by Lockheed.

In this report, the differences in the two approaches, that developed by ARL:UT for NASA, and that developed by Lockheed, are compared and conclusions are drawn with respect to NASA's options for achieving maximum potential from their digital synthetic aperture sensing system.

II. TASKS

A. Data Reduction

The original contract objectives included the processing of five radar images. Data were never provided to ARL:UT for processing, and what processing was done was performed by Lockheed at NASA, using rudimentary (and incorrect or incomplete) algorithms. The data tapes that were required by the contract were not supplied, and a decision was eventually made to relieve ARL:UT of this particular requirement.

B. Technology Transfer

Following two briefings by ARL:UT personnel for Lockheed/NASA personnel, one at NASA and one at ARL:UT, a correct analysis of the side-looking array radar (SLAR) digital data processing requirements was completed by NASA/Lockheed, with the exception of focus requirements and aperture weighting effects. However, Lockheed-generated software produced radar images of poor quality, and various improvements were suggested by ARL:UT personnel, which were not, unfortunately, based on a close liaison with Lockheed. Rather than implementing the ARL:UT developed algorithms, the major thrust seemed to be to attempt to correct the Lockheed developed software. Although meetings with Lockheed programmers were suggested, to try to comprehend their code, particularly the data handling routines, such meetings never occurred.

This report attempts to analyze potential problems in the Lockheed-developed software, deficiencies in the algorithms employed, or error sources in the parameters and data. Since no significant problems were encountered with data supplied to ARL:UT for development of the ground signal processor (GSP), it is assumed that the video data are good, and

that only errors in parameters (such as starting range sampling delay) are potential problems.

The significant changes that have reportedly been implemented in the initial software used by Lockheed are

1. application of weighting, or a "window", function to the synthetic array,

2. obtaining and applying the correct STC (sensitivity time control) delay to the transmit time, and

3. applying a focus algorithm to phase weight the data in the synthetic array.

Suggestions that have not been implemented are:

1. examine the mechanics of synthetic array overlay to ensure that near-identical Doppler filters are positioned at the same azimuth for each range sample,

2. add postprocessing algorithms

(1) to use the power in each sample, rather than signal (square root of power),

(2) to perform statistical analysis of the overlaid image array to determine mean, maximum, minimum, and standard deviation of the data,

(3) to establish a display noise threshold based on image statistics,

(4) after thresholding, to take the logarithm of the data, and make gray shade assignments based on a decibel scale and data dynamic range, and

(5) to display data in logarithmic form.

III. COMPARATIVE ANALYSIS OF DOPPLER CLUTTER SPECTRUM

In analyzing the requirements for reducing the raw video pulses recorded by the DDRS, the resolution to be achieved in the alongtrack, or azimuth dimension, must be considered. In theory, the so-called focused array can achieve a resolution of half the real antenna aperture. In practice, this is limited by the motion compensation and by the precision of the range to the start of sampling, as well as the focus corrections themselves.

In the case of the APQ-102/DDRS system, the delay to the start of sampling may be problematic, since the DDRS start time is delayed by an arbitrary value from the STC (sensitivity time control) trigger of the APQ-102, according to information supplied to ARL:UT by NASA. If the STC trigger time depends on the aircraft altitude (in order to maintain a constant minimum swath edge nadir angle of 14.2°, for example, in mode 1), the value for the RMIN range delay is readily known from the NASA Earth Resources Data Acquisition System (NERDAS) data for the aircraft altitude. Figures 1 and 2 indicate the geometry for the two radar modes available.

ARL:UT, at one point, was told that the STC trigger time could be represented as a linear function of altitude H (in feet) for each mode:

Mode	Algorithm	Units
1	0.00195 H + 7.68	μsec
2	0.00165 H + 69.5	μsec

Based on the mapping altitude of 60,550 ft in mode 1, the slant range for a nadir angle of 14.2° is 62,458 ft or a radar delay of 126.9 μsec (see Fig. 1). This is slightly more than the value of

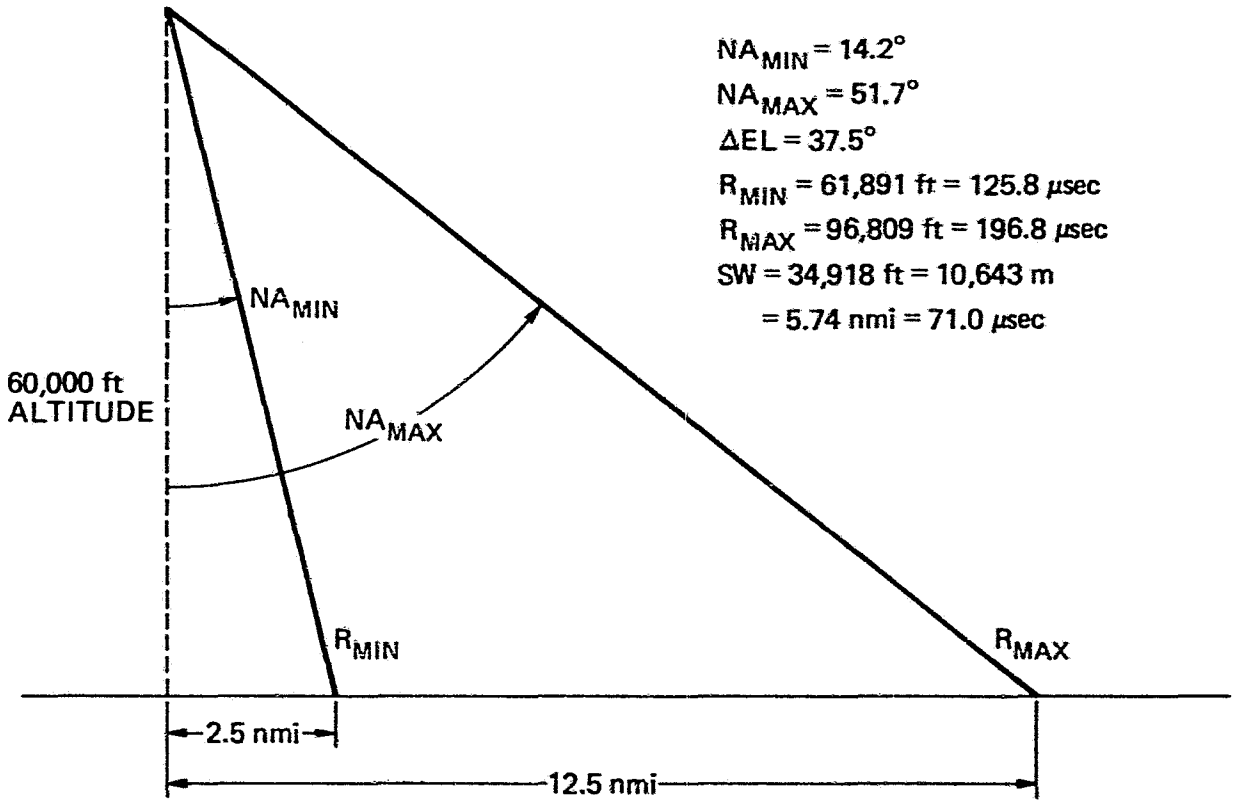

FIGURE 1
MODE 1 GEOMETRY

ARL-UT
AE-80-91
CRG-GA
9-11-80

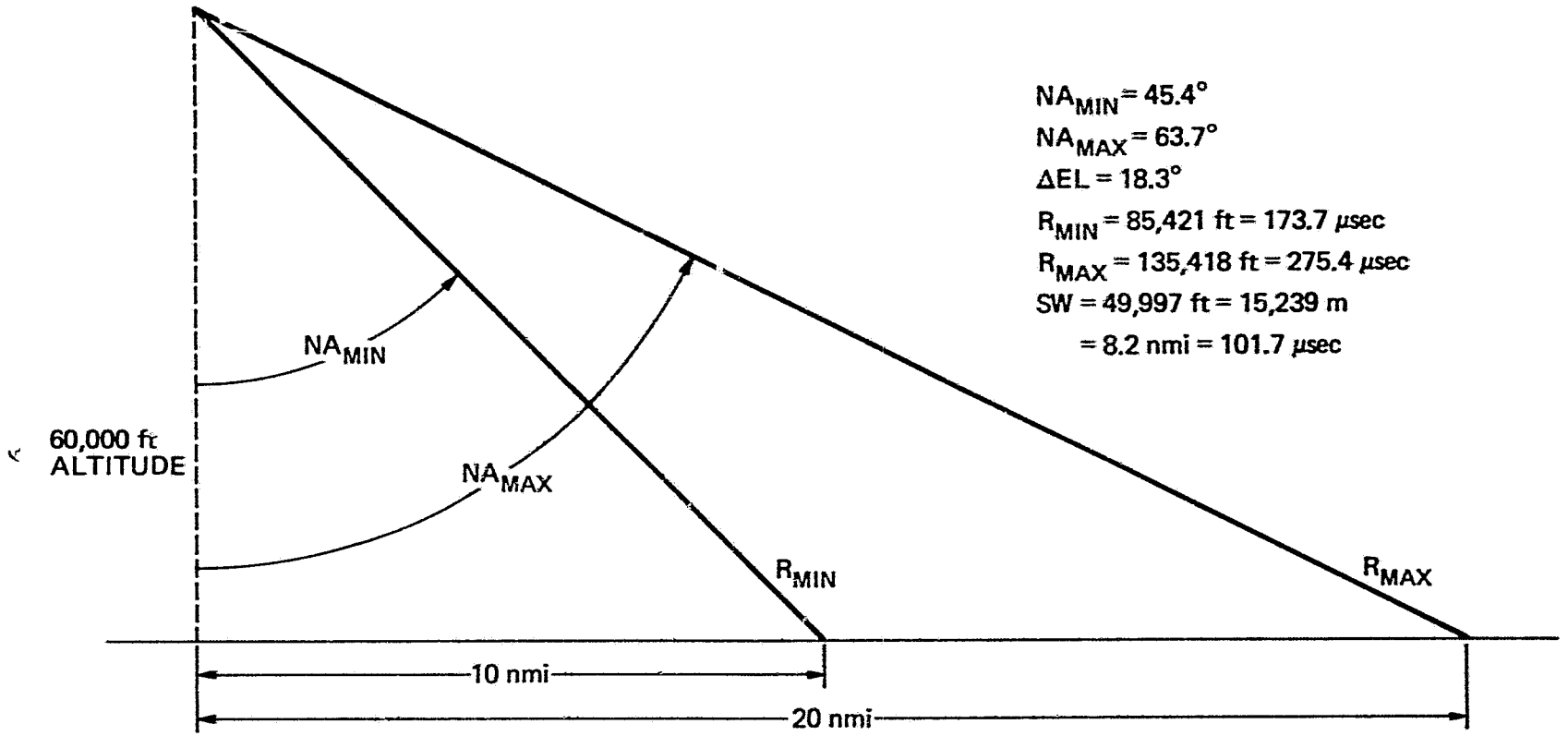

FIGURE 2
MODE 2 GEOMETRY

ARL:UT
AE-80-92
CRG-GA
9-11-80

125.8 μsec used in the ARL:UT GSP program for RMIN, which resulted in a satisfactory image. Using the algorithm, values are computed as follows.

Mode	Altitude (ft)	NA_{MIN}	Geometry Delay (μsec)	Algorithm Delay (μsec)
1	60,000	14.2°	125.8	124.68
2	60,000	45.4°	173.7	168.5
1	60,550	14.2°	126.9	125.75
2	60,550	45.4°	175.2	169.4

Although the algorithm has been determined to be in error, and is not now in use, the point is that the correct value of delay from transmit time to the start of sampling must be known, and significant errors (greater than 1 μsec) must be eliminated. This will be most apparent when the effect of a range error in the algorithms for Doppler filter width (array length) and for filter overlay is examined.

To assess the overall effectiveness of the correlations, it is good to first compare the two approaches in representing the usable Doppler spectrum.

A. NASA/Lockheed Representation

Appendix A is the approach to synthetic aperture radar (SAR) processing developed by NASA/Lockheed. Several comments are in order concerning these algorithms. First, considering the value of R_{MIN}, it should be pointed out that, for the DDRS initial sample, an additional increment of time DR_{MIN}, or delta R_{MIN}, is set by the operator, ranging from 2 to 99 μsec.

A second comment has to do with the maximum unfocused array length (see Section III of Appendix A). The definition is based on the allowable phase shift due to path length distance from one end of the array of pulses to be used to the other. This is arbitrarily taken to be 90°, $\pm\pi/4$ radians, with respect to the center of the array.

For an unfocused synthetic array of length L_{max}, the backscattered coherent pulses from a point target will add constructively with linear phase shift in time. Figure 3 illustrates this situation; if we want the phase shift corresponding to d to be less than 45° at each end of the array, relative to 0° in the middle, then

$$\frac{2\pi}{\lambda}\left[\sqrt{R_o^2 + \left(\frac{L_{max}}{2}\right)^2} - R_o\right] \leq \frac{\pi}{4} \quad , \tag{1}$$

and since $R_o^2 >> \left(\frac{L_{max}}{2}\right)^2$, d can be approximated with the first two terms in a binomial expansion as

$$R_o\left[1 + \frac{1}{2}\left(\frac{L_{max}}{2R_o}\right)^2\right] - R_o \quad ,$$

$$\left[\frac{R_o}{2}\left(\frac{L_{max}}{2R_o}\right)^2\right] \leq \frac{\lambda}{8} \quad . \tag{2}$$

Where the two sides are equal,

$$L_{max} = \sqrt{R_o \lambda} \quad , \tag{3}$$

a well-known result. Recalling that the synthetic aperture beamwidth is given by

$$\beta = \frac{\lambda}{2L} \quad , \tag{4}$$

the azimuth resolution at range R_o is

$$\rho_a = \beta R_o = \frac{R_o \lambda}{2L_{max}} \tag{5}$$

for the nonfocused case.

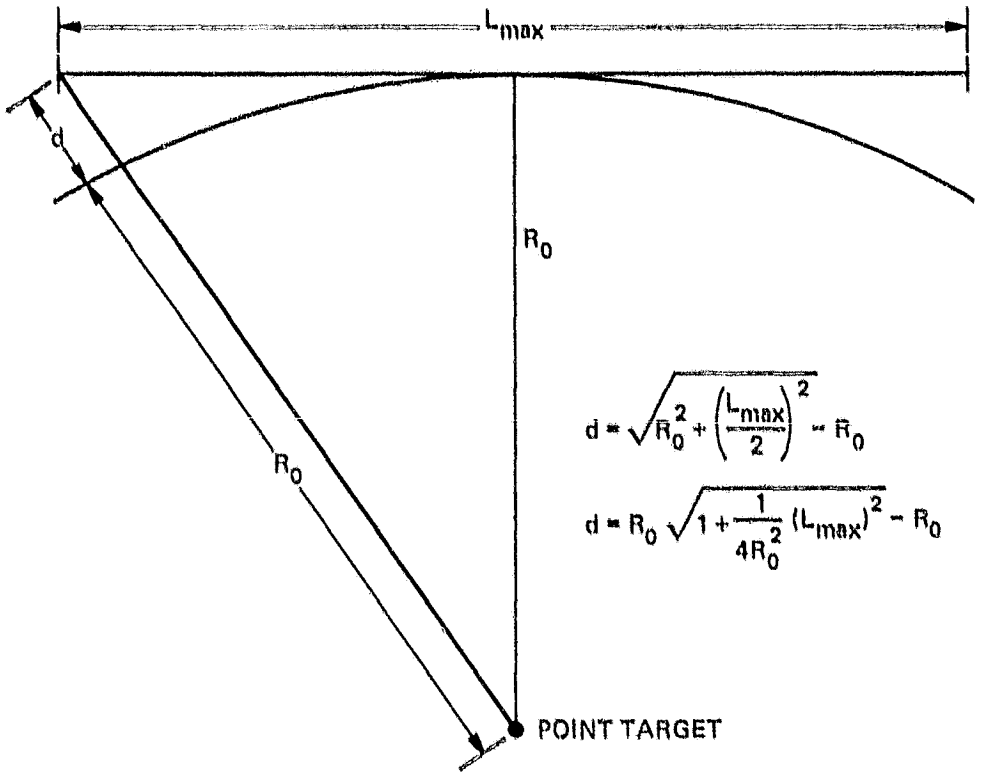

FIGURE 3
L_{max} FOR LINEAR FREQUENCY MODULATION

ARL:UT
AE-81-173
CRG - GA
12 - 1 - 81

In the APQ-102 mode 2, R_{MAX} is 136,402 ft, so that L_{max} = 118 ft (from Eq. (3) above) and the maximum number of pulses would be 236 (2 pulses per foot) for the unfocused array. At the closest range for mode 1, R_{MIN} = 62,875 ft, L_{max} = 80 ft, and the maximum number of pulses would be 160. If arrays of pulses greater in length than these are to be processed, some form of focusing or phase compensation for the end points in the array should be implemented. This process is performed in the optical processor used by Goodyear with a conical lens. The conical lens applies a phase taper as a function of position across the film strip in the azimuth direction, and it is also tapered in the range direction of the film to account for range variation of the focus function.

The digital processor implemented by ARL:UT for NASA converts the video samples to vectors by applying a unity valued vector with the appropriate phase rotation to each of the samples used in the synthetic array. A complex Fourier transform results in a complex Doppler filter output, and the magnitude is used to form the images.

In Fig. 4, if a point target is at x_o, y_o, z_o, and

$$R_o = \sqrt{x_o^2 + y_o^2 + z_o^2} \quad , \tag{6}$$

the two-way phase shift of an RF signal is

$$\phi(t) = -\frac{4\pi}{\lambda} R_o(t) \quad , \tag{7}$$

where R_o is the time dependent distance from the point target to the phase center of the radar. Then

$$R(t) = \sqrt{x_o^2 + (y_o - vt)^2 + z_o^2} \quad . \tag{8}$$

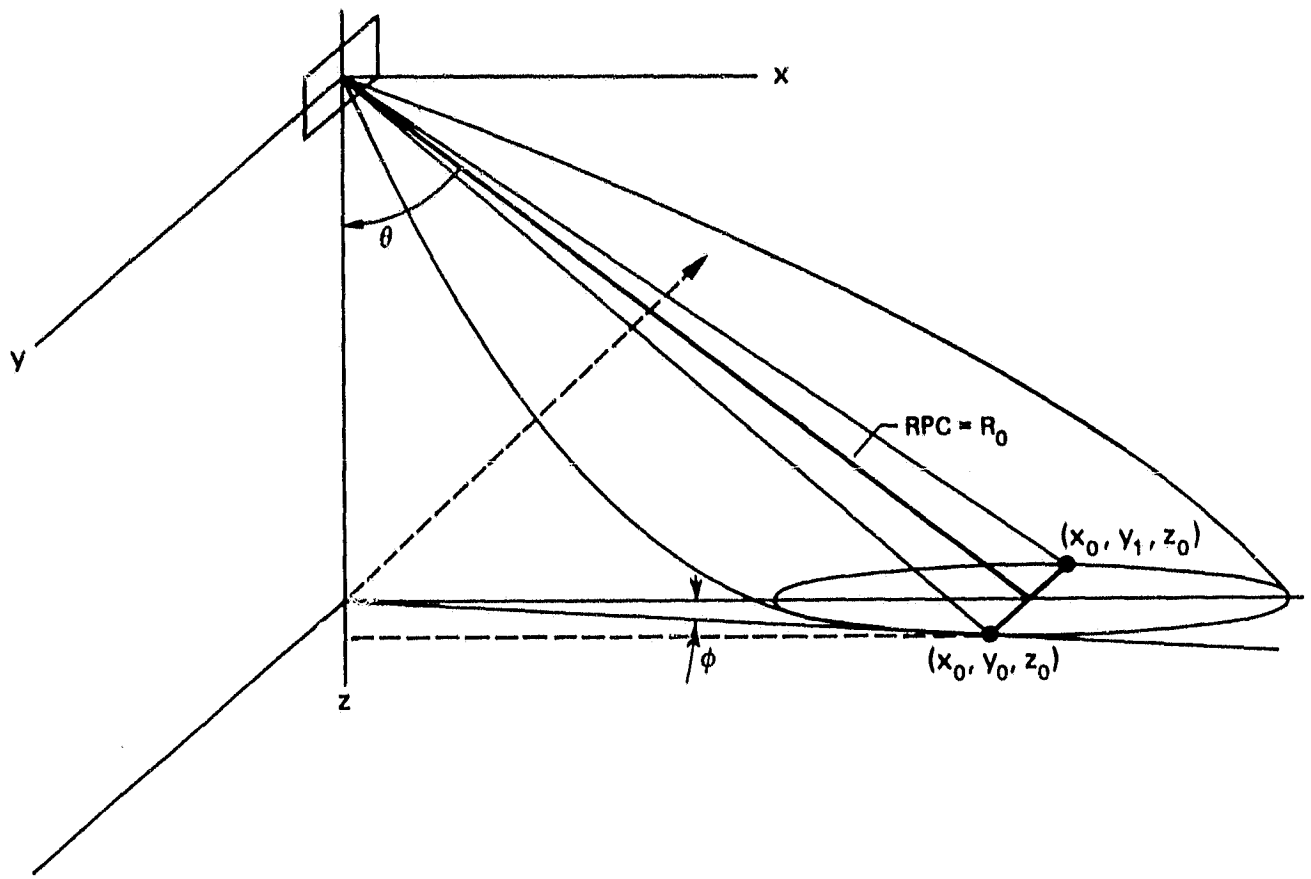

FIGURE 4
APQ-102 GEOMETRY

ARL:UT
AE-81-172
CRG - GA
12 - 1 - 81

Expanding the function R(t) about the point R_o (using McLaurin's series for the derivatives) gives

$$R(t) = R_o \left[1 - \frac{y_o v t}{R_o^2} + \frac{1}{2} \left(1 - \frac{y_o^2}{R_o^2} \right) \frac{v^2 t^2}{R_o^2} + \ldots \right] \quad . \tag{9}$$

The reflected signal from the point target is

$$F(t) = a(t) \cos\left[w_o t - \frac{4\pi}{\lambda} R(t) \right]$$

$$= a(t) \cos\left[w_o t - \frac{4\pi}{\lambda} R_o + \frac{4\pi}{\lambda} \frac{y_o v}{R_o} t - \frac{4\pi}{\lambda} \frac{1}{2} \left(1 - \frac{y_o^2}{R_o^2} \right) \frac{v^2}{R_o} t^2 + \ldots \right] \quad . \tag{10}$$

This applies during the period of time the point target is illuminated by the real beam, i.e., from y_o to y_1, and is called the aperture integration time,

$$T_a = \frac{y_o - y_1}{v} \quad .$$

The terms in Eq. (10) correspond to a constant phase shift, a constant Doppler frequency (linear phase shift with time), and a linear FM (quadratic phase shift with time). This last coefficient is

$$m_d = - \frac{2\pi}{\lambda} \frac{v^2}{R_o} \left(1 - \frac{y_o^2}{R_o^2} \right) \quad , \tag{11}$$

and it is centered on

$$w_d = \frac{4\pi}{\lambda} \frac{y_o v}{R_o} \quad .$$

There are, of course, higher order terms, which can be ignored in the analysis. Putting these results in spherical coordinates,

$$\frac{y_o}{R_o} = \sin\theta \cos\phi \quad , \tag{12}$$

and

$$m_d = -\frac{2\pi}{\lambda}\frac{v^2}{R_o}(1-\sin^2\theta\cos^2\phi) \quad ; \tag{13}$$

also,

$$w_d = \frac{4\pi}{\lambda} v \sin\theta \cos\phi \quad . \tag{14}$$

The Doppler bandwidth is

$$\Omega = T_A m_d = |y_o - y_1| \frac{2\pi}{\lambda}\frac{v}{R_o} |(1-\sin^2\theta\cos^2\phi)| \quad . \tag{15}$$

The Doppler spectrum amplitude is, excluding the RF spectrum,

$$A(w) = a\left(\frac{w}{m_d}\right) \quad , \quad \text{for } |w| \leq \frac{\Omega}{2} \quad , \tag{16}$$

and is affected by the real antenna beam shape which sets a(t), as well as the target radar cross section σ. For the SLAR case ϕ=0, and

$$\Omega = |y_o - y_1| \frac{2\pi}{\lambda}\frac{v}{R_o} \cos^2\theta \quad . \tag{17}$$

provided $|y_o - y_1|$ is less than $R_o\beta$, where β is the 3 dB beamwidth of the real antenna beam.

Thus it is necessary to take into account the FM rate of the Doppler returns, m_d, since it depends on the range R_o and the angle θ.

The phase shift from the center of the aperture length to one end is

$$\Delta\phi = \frac{1}{2} m_d \left(\frac{T_A}{2}\right)^2 = \frac{m_d T_A^2}{8} \quad . \tag{18}$$

To keep $\Delta\phi$ less than $\pi/4$ as a limit,

$$-\frac{4\pi}{\lambda}\frac{v^2}{R_o}\cos^2\theta\,\frac{T_A^2}{8} + \frac{4\pi}{\lambda}\frac{v^2}{R_o - \Delta R}\cos^2\theta\,\frac{T_A^2}{8} \leq \frac{\pi}{4} \quad , \tag{19}$$

or

$$\frac{1}{R_o + \Delta R} - \frac{1}{R_o} \leq \frac{2\lambda}{\left(T_A v\cos\theta\right)^2} \quad , \tag{20a}$$

and, to the other end,

$$\frac{1}{R_o} - \frac{1}{R_o + \Delta R} \leq \frac{2\lambda}{\left(T_A v\cos\theta\right)^2} \quad , \tag{20b}$$

$$\frac{\Delta R}{-R_o(R_o - \Delta R)} \leq \frac{2\lambda}{\left(T_A v\cos\theta\right)^2} \quad , \tag{21a}$$

$$\frac{\Delta R}{R_o(R_o + \Delta R)} \leq \frac{2\lambda}{\left(T_A v\cos\theta\right)^2} \quad , \tag{21b}$$

and, assuming

$$R_o^2 > R_o \Delta R \quad ,$$

$$|\Delta R| \leq \frac{2\lambda R_o}{\left(T_A v\cos\theta\right)^2} \quad .$$

The depth of the focus F_D is defined as 2R,

$$F_D = \frac{4\lambda R_o}{\left(T_A v \cos\theta\right)^2} = \frac{4\lambda R_o}{\left|y_o - y_1\right|^2 \cos^2\theta} \quad . \tag{22}$$

If we express the real beam coverage $|y_o - y_1|$ in terms of pulses, we have $N_p = 2|y_o - y_1|$ in feet, so that, for the APQ-102,

$$F_D = \frac{16\lambda R_o}{N_p^2 \cos^2\theta} \quad .$$

For the case of the APQ-102 operated in mode 1, 7-bit precision, 512 range bins recorded, and a start sampling delay of 2 μsec, we might assume a value for R_o of 79,384 ft, λ = 0.1025 ft. For this case, θ=40.9° and

$$F_D = \frac{227877}{N_p^2} = 3.5 \text{ ft for 256 pulses,} \quad 55.6 \text{ ft for 64 pulses.}$$

If we relax our criterion for the allowable phase shift to $\pi/2$ at each end of the synthetic array, so that

$$\frac{1}{R_o} - \frac{1}{R_o + \Delta R} \leq \frac{\lambda}{\left(T_A v \cos\theta\right)^2} \quad , \tag{23}$$

$$|\Delta R| \leq \frac{\lambda R_o}{\left(T_A v \cos\theta\right)^2} \quad , \tag{24}$$

and

$$F_D = \frac{8\lambda R_o}{N_p^2 \cos^2\theta} \quad , \tag{25}$$

the depth of the field is cut in half.

It is apparent that for long arrays of pulses, the depth of field is very limited, and focusing is advisable. The APQ-102 coherently detects the bipolar video levels and records the in-phase components on film relative to a neutral gray shade corresponding to zero value of the in-phase component of the video. These same values are converted by the DDRS into 7-, 4-, or 2-bit levels, Miller encoded, and recorded on a wideband tape recorder.

The data can then be focused by applying a phase shift function, which effectively converts each value to a complex number. A complex Fourier transform produces a filter spectrum containing positive and negative coefficients, centered at PRF/4. The filter magnitudes are formed by discarding the negative values, which have no physical significance, being merely artifacts of the focusing operation.

A second and important consideration in the NASA version of a data azimuth (Doppler) correlator is the use of a weighting function. The generalized ambiguity function in the crossrange direction has -13.2 dB first sidelobes and a -3 dB main lobe (half-power) of 0.886/B in the Doppler frequency domain, where B is the length of the array in time, or half the number of pulses (feet) divided by the aircraft velocity. In other words, a uniformly weighted array of data points results in a sinx/x transformed pattern. To improve the sidelobe structure (reduce it), thus reducing sidelobe interference, aperture weighting is employed. Table I[1] gives some typical performance parameters.

Use of weighting results in main beam broadening and consequent decreased resolution. This broadening must be taken into account when performing coherent integration of corresponding spectral filters from successive data arrays. Although the NASA/Lockheed correlator uses the Kaiser weighting function, it is not clear that the beam broadening effect is taken into account in the algorithms in the software that perform the overlaying, or integration.

TABLE I

PERFORMANCE FOR VARIOUS FREQUENCY-WEIGHTING FUNCTIONS

	Weighting function	Pedestal height H, %	SNR loss, db	Mainlobe width, −3 db	Peak sidelobe level, db	Far sidelobe falloff
1	Uniform	100	0	$0.886/B$	−13.2	6 db/octave
2	Dolph-Chebyshev	.....	....	$1.2/B$	−40	No decay
3	Taylor ($\bar{n} = 8$)	11	1.14	$1.25/B$	−40	6 db†/octave
4	Cosine-squared plus pedestal: $H + (1 - H)\cos^2(\pi f/B)$					
	a. Hamming	8	1.34	$1.33/B$	−42.8	6 db/octave
	b. 3:1 "taper ratio"	33.3	0.55	$1.09/B$	−25.7	6 db/octave
5	$\cos^2(\pi f/B)$	0	1.76	$1.46/B$	−31.7	18 db/octave
6	$\cos^3(\pi f/B)$	0	2.38	$1.66/B$	−39.1	24 db/octave
7	$\cos^4(\pi f/B)$	0	2.88	$1.94/B$	−47	30 db/octave
8	Triangular: $1 - 2\lvert f\rvert/B$	0	1.25	$1.27/B$	−26.4	12 db/octave

† In the region $|t| > 8/B$.

(This table was reproduced from Radar Handbook, M. I. Skolnik (Ed.).)

In determining the azimuth resolution, the important consideration is the shape of the main lobe of the Doppler filter, determined by convolving the "window" function and the uniform distribution of length equal to the observation time. The resulting filter shape using, for example, the Taylor weighting function with -30 dB first sidelobes, is calculated to broaden the -3 dB response by a factor of 1.27. Figure 5 illustrates the situation. Figure 5(a) shows the -3 dB resolution of the filter shape for an unweighted (uniform) collection of sampled data (radar pulses) of a given length. Figure 5(b) shows what happens to the spectral response after weighting the samples in the time series. Because of the finite length of the sample, an array of these responses is produced, as illustrated in Fig. 5(c). The response spacing is set by the observation time, or alternatively, by the number of pulses times the interpulse period or sampling interval.

Thus, except for a unique combination of observation time and window beam broadening factor, the effective linear measure of real estate corresponding to α, called RESA (the filter width at the -3 dB points), will not be equal to the Doppler sample spacing. The sampling ratio (SR), defined as SR=RESA/sample spacing, is a measure of the information content in the image. Specific values of SR should be obtained based on user requirements and/or display criteria.

This means that, in calculating the coverage of each successive array of pulses at a given range, the distance moved by the real antenna, equal to half the number of pulses in feet, must be converted to an equivalent number of Doppler resolution cells for a particular range.

Concerning the analysis of the problem by NASA/Lockheed (Appendix A), the following comments are in order. First, it is intended to restrict the size of arrays processed so that focusing is not necessary. As a matter of convenience, however, standard length arrays of 256 or 512 pulses are Fourier processed, and defocusing takes place.

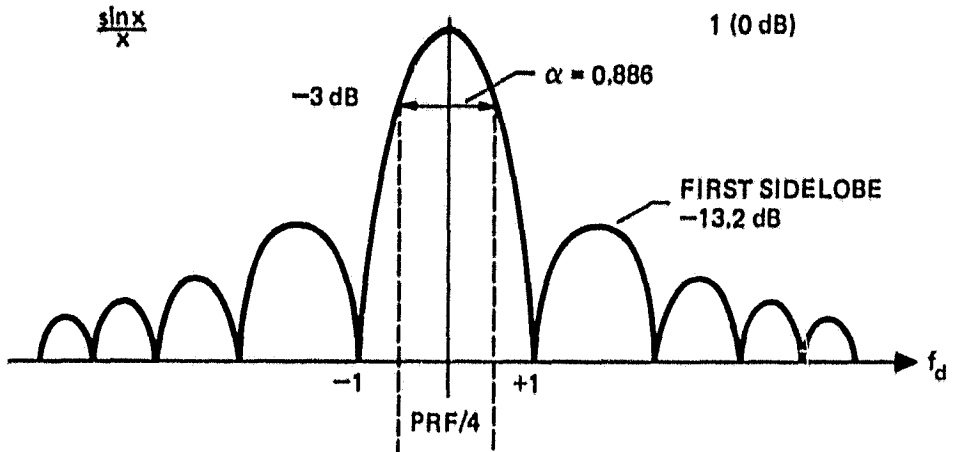

(a) TRANSFORM FUNCTION OF A RECTANGULAR FUNCTION (UNIFORM)

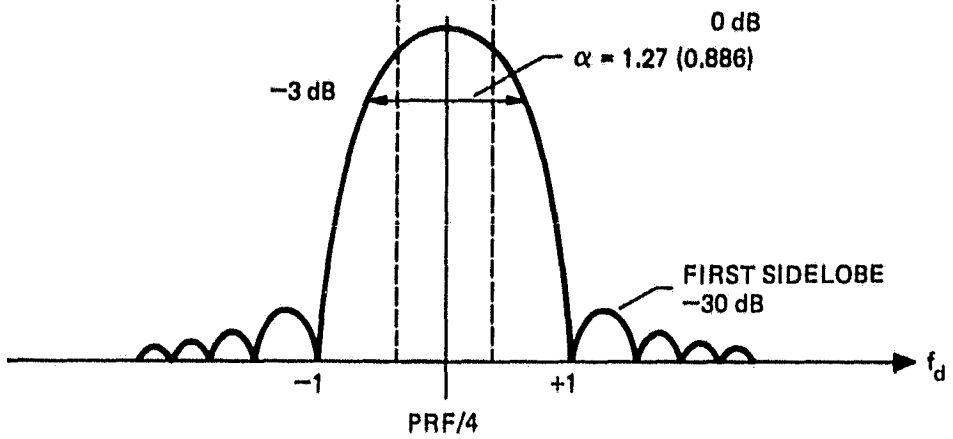

(b) RESPONSE AFTER WEIGHTING, OR "WINDOWING" (30 dB TAYLOR)

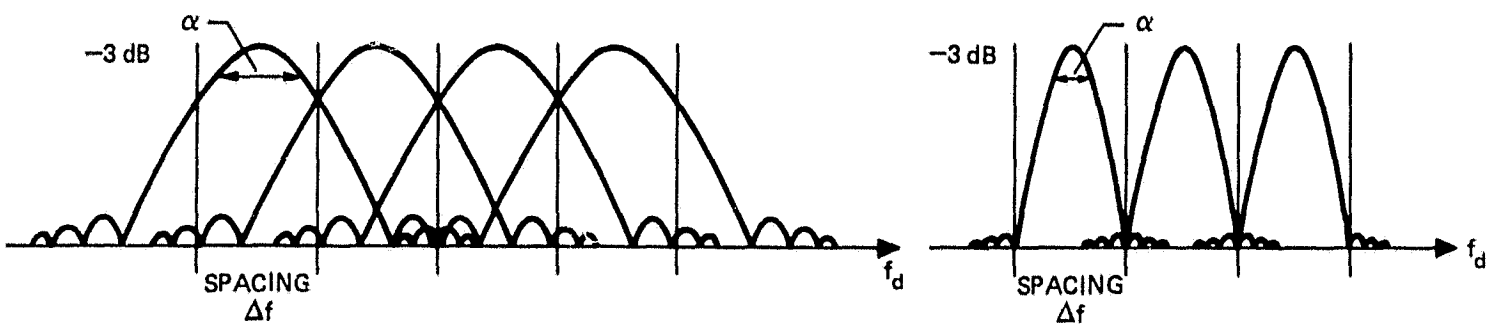

(c) FILTER SPACING versus RESOLUTION α

FIGURE 5
DOPPLER TRANSFORM FUNCTIONS

ARL:UT
AE-81-174
CRG - GA
12 - 1 - 81

In Section III of Appendix A, the following statement is made:

> "Since the FFT is in the frequency domain, thus each bin (filter component) is:
>
> $$\Delta_f = PRF/N_p \quad ."$$

According to sampling theory, the resolution of a sample space linear series in the transform domain is no greater than the reciprocal of the observation period and, for real valued series, the highest recoverable component is half the sample rate.

This means that by using zero to fill in the pulse sample series, any arbitrary resolution may be obtained in the Doppler filter spacing, a feature useful in maintaining a given aspect ratio with respect to the range dimension of a pixel in the image display. Conversely, using more general Fourier transform algorithms, a series of arbitrary length may be chosen to obtain a desired filter resolution in the Doppler domain.

It should be pointed out that the "usable Doppler" of Appendix A, Section III, is defined as the Doppler bandwidth encompassed by the 3 dB beamwidth of the real antenna. On the following page, the usable Doppler is also defined as PRF/4 ± 1/2 the usable Doppler, i.e., the 3 dB beamwidth Doppler is shifted from zero frequency to center it on PRF/4, since this is the output of the APQ-102 receiver detection system.

The following statement is made in Section IV:

> "Since a primary consideration is the focused part of the beam at anyone (sic) given time, then, the total number of filters which represent it are:
>
> $$J = D_f/FT \quad ."$$

The approach taken is to select, from an unfocused long synthetic array transform those Doppler filters in the central portion of the real beam coverage, and assume that they meet the criterion for depth of

field. This is incorrect, since these filters may contain contributions from phase shifted scatterers at the edges of the real beam coverage for the beginning and end points of the synthetic array.

The proper approach, of course, is to either focus the array prior to transformation, or suitably restrict its length.

Attempts to adjust the focal point for the different ranges to compensate for the lack of depth of field will not be successful, using the NASA/Lockheed approach.

B. ARL:UT Representation

In the ARL:UT derived GSP routines, the azimuth filter spacing is usually required to be the same as the range spacing at the patch center range, and the azimuth resolution is the same as the range resolution, RESA-RESR, at each range bin. The range resolution algorithm is the same as in Appendix A. It is instructive to show that the analyses are the same, using the notation of Appendix A, Section III.

$$D_{zero} = PRF/4 \quad ; \quad D_F = \sqrt{\lambda R_{pc}}$$

$$D_{op} = \frac{2V_r}{\lambda} = \frac{2V \cdot c \sin B_w}{\lambda} \approx \frac{2VB_w}{\lambda} \quad ; \quad B_w = 1.3^\circ$$

$$D_{op}/2 = \frac{VB_w}{\lambda} \quad ; \quad D_{zero} = \frac{PRF}{4} \quad ; \quad D_u = D_{zero} \pm D_{op}/2$$

$$D_u = PRF/4 \pm \frac{VB_w}{\lambda} \quad ; \quad \Delta f = \frac{PRF}{N_p} \quad .$$

$$I_S = \left(\frac{PRF}{4} - \frac{VB_w}{\lambda}\right)\frac{N_p}{PRF} \quad ; \quad I_E = \left(\frac{PRF}{4} + \frac{VB_w}{\lambda}\right)\frac{N_p}{PRF} \quad . \quad (26)$$

From Section IV,

$$M = I_E - I_S + 1 = \frac{N_p}{PRF}\left(\frac{2VB_w}{\lambda}\right) + 1 \quad , \tag{27}$$

the number of filters in the real aperture.

$$FT = \frac{B_w \cdot R_{pc}}{M} \quad ; \quad M \cdot FT = B_w \cdot R_{pc} \quad , \tag{28}$$

$$J = \frac{D_f}{FT} \quad ; \quad D_f = J \cdot FT = JB_w \cdot R_{pc} \Big/ M \quad ;$$

therefore,

$$M\sqrt{\lambda R_{pc}} = J \cdot B_w \cdot R_{pc} \quad , \tag{29}$$

and

$$M = J \cdot B_w \sqrt{\frac{R_{pc}}{\lambda}} \quad ; \quad J = \frac{M}{B_w}\sqrt{\frac{\lambda}{R_{pc}}} \quad . \tag{30}$$

Substituting for M,

$$J = \left[\frac{N_p}{PRF}\left(\frac{2VB_w}{\lambda}\right) + 1\right]\sqrt{\frac{\lambda}{R_{pc}}}\,\frac{1}{B_w}$$

$$= \frac{2N_pVB_w + PRF \cdot \lambda}{PRF\sqrt{\lambda R_{pc}}}\,\frac{1}{B_w} = \frac{2N_pVB_w}{B_wPRF\sqrt{\lambda R_{pc}}} + \frac{\lambda}{B_w\sqrt{\lambda R_{pc}}} \quad . \tag{31}$$

$$J \simeq \frac{N_p 2V}{PRF \cdot \lambda}\sqrt{\frac{\lambda}{R_{pc}}} \quad . \tag{32}$$

Since, in effect, the PRF is two pulses per foot of platform travel,

$$J = \frac{N_p \cdot 2V}{2p/ft \cdot V\ ft/sec} \frac{1}{\sqrt{\lambda R_{pc}}} = \frac{N_p}{\sqrt{\lambda R_{pc}}} \quad . \qquad (33)$$

This shows that essentially the same formulation is being used by the ARL:UT approach in determining the unfocused achievable resolution. As pointed out above, the improper implementation by Lockheed/NASA results in a defocused image. Also, use of the approach in the Lockheed/NASA software can result in the introduction of additional errors. The first thing that is done using the Lockheed/NASA approach is to calculate the PRF as the reciprocal of twice the ground speed in ft/sec; whereas this is correct for the first few arrays formed, the ground speed of the plane may change 5% during the time required for image formation. This error, depending upon the other parameters, could result in much larger errors of filter spacing, and thus image resolution would be degraded with overlay.

The ARL:UT formulation is given in the technical report ARL-TR-81-21, "Development of a Ground Signal Processor for Digital Synthetic Array Radar Data," 22 May 1981; other considerations, such as beam broadening versus filter spacing, accuracy of filter overlay, and selection of N_p to achieve desired pixel dimensions, are discussed in that report.

IV. RESULTS

The APQ-102 radar images produced by the Lockheed algorithms are defocused (smeared) and create blooming problems on a CRT display. The blooming is due to the data being supplied in a linear format. The concluding sentence in Appendix A is

> "The data referred to is the square root of the real and imaginary pair squared amplitude of the pixel."

The proper representation should be the power in the pixel, and preferably the logarithm of the power, with suitable thresholds to remove noise and adjust the dynamic range of the data to the dynamic range of the display. Postprocessing could include a statistical analysis of the filter data to establish the thresholds and the gray shade assignments.

As discussed in Section III, there are three possible major error sources.

1. Incorrect or inaccurate range data (timing delay).
2. Uncompensated synthetic arrays exceeding the allowable length for the nonfocused case.
3. Improper registration or overlay of filters (azimuth lines) due to incorrect data handling in the overlay process or error propagated in the computation of various parameters.

Appendix B, produced by Lockheed personnel, indicates an attempt to address this last item, although the approach is purely empirical, or a "cut and try" type of solution.

The discussions of antenna beam shape are particularly confusing, since the antenna beam shape is known to be sinx/x in azimuth, and has

in fact been measured. The filter shape of the Doppler filters can be derived once the weighting function is chosen, or it can be determined from measurements. The discussion in Appendix B seems to indicate a lack of understanding of the relationships between range and the iso-Doppler lines of the image.

APPENDIX A

SAR PROCESSING (NASA/LOCKHEED)

SAR PROCESSING

I. The following method is employed to determine the (R_{pc}) range to the patch center. Clearly

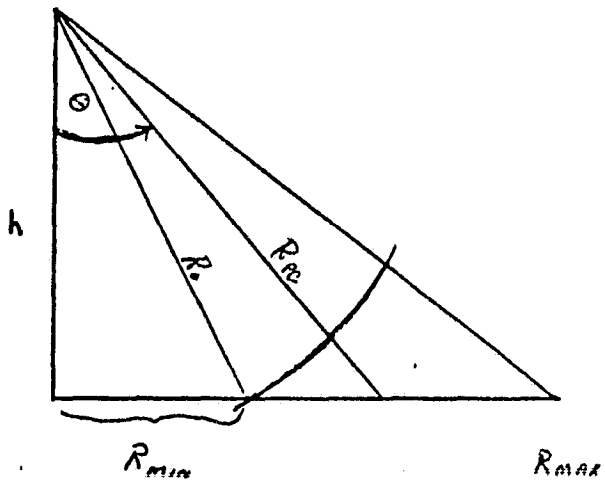

$$R_o = \sqrt{h^2 + R^2_{min}}$$

where

R_{min} = 2.5 Nm or 10 Nm

dependent upon a mode setting of the radar

The parameter R_{max} is found by adding to R_{min} the following parameter

$$N_{RB}\ S_I\ C/2$$

where

N_{RB} - the maximum number of range bins used

S_I - the sample interval sample rate in seconds

C - the speed of light

2 - a factor used to denote both sending and receiving a signal

The parameter R_{pc} is found by changing the division factor to 4.

II. The slant range resolution is found by the following manner

$$R_{SL} = C \cdot S_I / 2$$

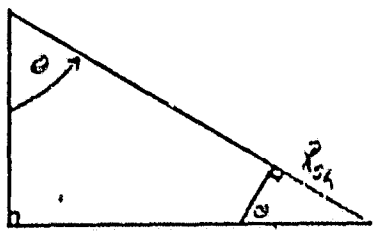

$$\frac{R_{SL}}{\sin\theta} = \frac{R_{GRND}}{1}$$

$$R_{GRND} = R_{SL}/\sin\theta$$

III. Azimuth Filter determination

The FFT once evaluated yields a frequency image of the real aperture; however a characteristic of the system which must be kept in mind is that the doppler data is offset. By definition, the maximum distance in the beam which may be considered as focused is:

$$D_f = \sqrt{\lambda R_{pc}}$$

Since the data is encoded in PCM form at a rate of 2 pulses per foot, then clearly the number of required pulses is:

$$N_p = 2 D_f$$

Assume an FFT may be found (some power of 2) which contains data which is $\leq 2 D_f$ and

$$\hat{N}_p = 2 D_f - \Delta$$

The usable doppler bandwidth is:

$$D_{op} = \frac{2V \cdot C \cdot \sin B_W}{\lambda}$$

where

B_W - real beam width (1.3°)
C - a conversion constant
λ - wavelength

The zero doppler is:

$$D_{zero} = PRF/4$$

The usable doppler is:

$$D_u = D_{zero} \pm D_{op/2}$$

Since the FFT is in the frequency domain, thus each bin (filter component) is:

$$\Delta_f = PRF/Np$$

The indices which point to the usable doppler are:

$$I_S = D_u(-)/\Delta_f$$

$$I_E = D_u(+)/\Delta_f$$

IV. Filter Overlaying

From section 2 the total number of filters representing the real aperture is:

$$M = I_E - I_s + 1$$

This is representative of X number of feet per bin on the ground as:

$$FT = B_w \cdot R_{pc/m}$$

Since a primary consideration is the focused part of the beam at anyone given time, then, the total number of filters which represent it are:

$$J = D_{f/FT}$$

In order to line up successive FFT's the transform must slide in time by J·FT·2 pulses. This implies that the overlay is incremented J bins in azimuth for a processed range bin.

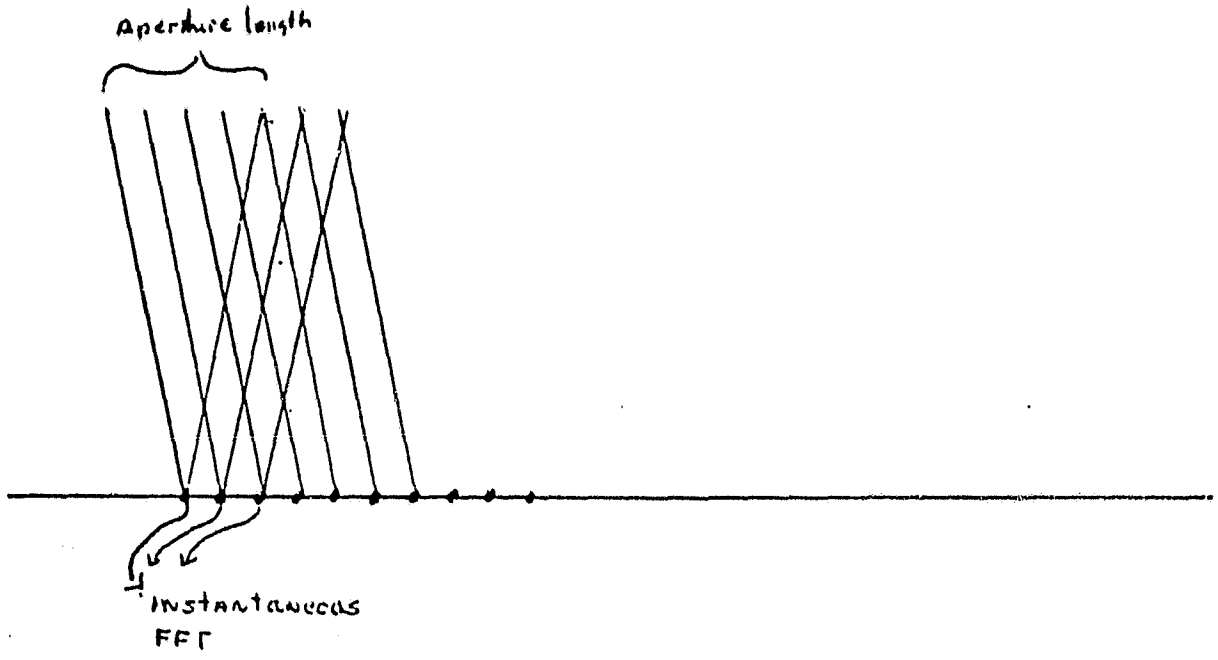

The basic philosophy is that if you slide X feet in pulses (shift), it also shifts X feet in the aperture. Once shifted, the aperture region in common with each other may be simply added.

The resultant summation of these data may then be output as an image pixel. (The data referred to is the square root of the real and imaginary pair squared amplitude of the pixel).

APPENDIX B

SAR PROCESSING (LOCKHEED)

SAR PROCESSING

Two basic problems have been investigated for the SAR processing. First the type or window functions used was made optional, and are

1. Cosine
2. Kaiser
3. Taylor

A characteristic of these functions are that the Kaiser window tends to have a smaller standard deviation from the mean than either the Taylor or Cosine. The Taylor window provides a smaller standard deviation than the Cosine.

The second problem addressed involved overlaying to reduce focusing problems at the near and far range bins. By making a modification to permit, if desired, the number of pulses used for overlaying variable then parametric runs have been generated.

- CASE 1 - Using a constant 1.3° beam width, and, the same number of pulses in the near and far range to overlap a control case was generated.

- CASE 2 - Using a constant 1.3° beam width, (the angle to the near and far range bins was assumed to be 1.3°) the respective width of the real antenna beam width was computed and used. In this case 68/97 pulses were slide for the near and far range bins.

- CASE 3 - Using the results from CASE 2, the width of the beam was increased at the near bin to 1.5° and the far end was decreased to 1.25°. This effectively increased the pulses to slide during overlaying over case 1 at the extreme ends.

The algorithm used to compute the real aperture is:

$$l = 2r \tan \Psi/2$$

for small angles $\tan \Theta = \Theta$

$$l = 2r \Psi/2 = r4$$

where Ψ = the beam width of the antenna

As long as the angle l is to the patch center, this does not seem to generate any problem. However, to yield a constant slice of real estate indicate that the near angle is > than the middle > the far angle. However, it seems somewhat intuitive that the antenna pattern is not really rectangular in shape, but probably better modeled as a trapozoid. This would permit the angle to the main lobe to be 1.3°, the angle at the near end > 1.3° and for end = 1.3°.

Analysis of Results

- CASE 1 - generates a reasonable picture, but the near and far bins tends to be out of focus. (smeared)
- CASE 2 - smears the near range bins and tends to focus the far end.
- CASE 3 - has positive results with the focusing of data at the near end and far end. The near end bin is not as good as in CASE 1, the far end is better.

The real aperture length at the near range bin is assumed $\sim r_1\Psi$ and at the far end $r_2\hat{\Psi}$ where r_1, r_2 represent range at the near and far end of the image. It is assumed that $\hat{\Psi} \geq \Psi$.

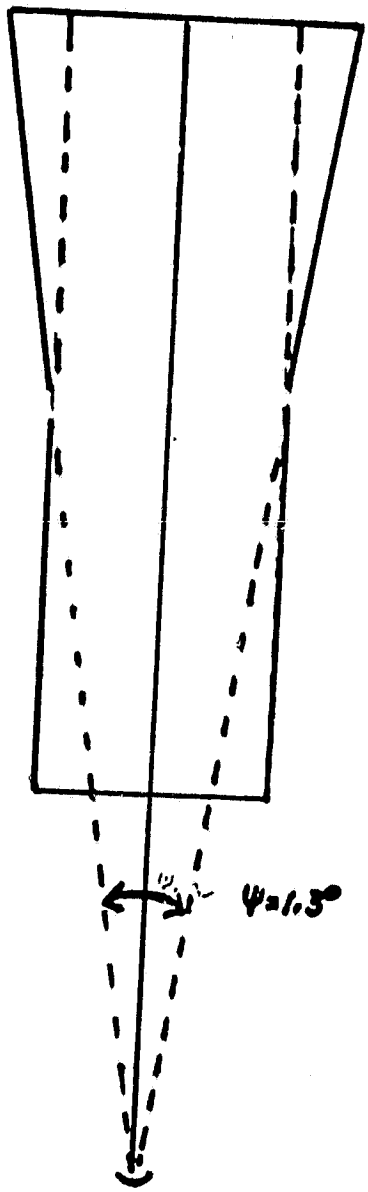

Antenna Pattern on ground

REFERENCES

1. M. I. Skolnik (Ed.), Radar Handbook (McGraw Hill Book Co., Inc. New York, 1970).